MARSIS surface reflectivity of the south residual cap of Mars

Jeremie Mouginot, W. Kofman, A. Safaeinili, C. Grima, A. Null Herique, J.J. Plaut

Accepted Manuscript

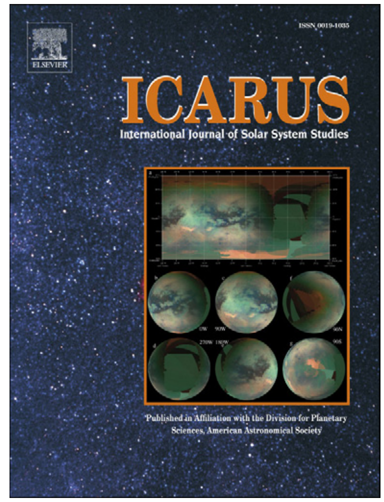

MARSIS surface reflectivity of the south residual cap of Mars

Jeremie Mouginot, W. Kofman, A. Safaeinili, C. Grima, A. Herique, J.J. Plaut

PII: S0019-1035(09)00031-1
DOI: 10.1016/j.icarus.2009.01.009
Reference: YICAR 8891

To appear in: *Icarus*

Received date: 1 July 2008
Revised date: 16 October 2008
Accepted date: 9 January 2009

Please cite this article as: J. Mouginot, W. Kofman, A. Safaeinili, C. Grima, A. Herique, J.J. Plaut, MARSIS surface reflectivity of the south residual cap of Mars, *Icarus* (2009), doi: 10.1016/j.icarus.2009.01.009

MARSIS surface reflectivity of the south residual cap of Mars

Mouginot J.[1], (jeremie.mouginot@obs.ujf-grenoble.fr)

Kofman W.[1], (wlodek.kofman@obs.ujf-grenoble.fr)

Safaeinili A.[2], (ali.safaeinili@jpl.nasa.gov)

Grima C.[1], (cyril.grima@obs.ujf-grenoble.fr)

Herique A.[1], (alain.herique@obs.ujf-grenoble.fr)

Plaut J. J.[2] (plaut@jpl.nasa.gov)

[1]Laboratoire de Planétologie de Grenoble, CNRS/UJF 38041 Grenoble Cedex, France

[2]Jet Propulsion Laboratory, California Institute of Technology, Pasadena, CA 91109.

Manuscript : 13 pages

Figures : 5 pages

Tables : 1 page

Proposed running head:

MARSIS surface reflectivity of the South Residual Cap.

The name and address to which editorial correspondence and proofs should be directed:

Jeremie MOUGINOT
122 rue de la piscine
38000 Grenoble
FRANCE
Jeremie.mouginot@obs.ujf-grenoble.fr

(Abstract)

The south residual cap of Mars is commonly described as a thin and bright layer of CO_2-ice. The Mars Advanced Radar for Subsurface and Ionospheric Sounding (MARSIS) is a low-frequency radar on board Mars Express operating at the wavelength between 55 and 230 m in vacuum. The reflection of the radar wave on a stratified medium like the residual cap can generate interferences, causing weaker surface reflections compared to reflections from a pure water ice surface.

In order to understand this anomalous low reflectivity, we propose a stratified medium model, which allows us to estimate both the thickness and the dielectric constant of the optically thin slab. First, we consider the residual cap as single unit and show that the decrease in the reflected echo strength is well explained by a mean thickness of 11 m and a mean dielectric constant of 2.2. This value of dielectric constant is close to the experimental value 2.12 for pure CO_2-ice. Second, we study the spatial variability of the radar surface reflectivity. We observe that the reflectivity is not homogeneous over the residual cap. This heterogeneity can be modeled either by variable thickness or variable dielectric constant. The surface reflectivity shows that two different units comprise the residual cap, one central unit with high reflectivity and surrounding, less reflective units.

KEYWORD: RADAR OBSERVATIONS, MARS, POLAR CAPS, ICES

1. Introduction

1.1. South residual cap

The south polar plateau of Mars is partially covered by a perennial thin layer of carbon dioxide (CO_2) ice, which is easily visible from Earth and spacecraft due to its high albedo compared to the surrounding regions. Astronomers have observed this layer over a century [Flammarion 1892], but the composition (CO_2-ice) was determined using Viking orbiter thermal data [Kieffer, 1979; Paige *et al.* 1990]. It has been shown that this CO_2 layer directly lies above water ice (H_2O-ice), which comprises the major part of the plateau [Plaut *et al.* 2007] in the form of South Polar Layered Deposits (SPLD).

Thermal data from Thermal Emission Imaging System (THEMIS) revealed the presence of small exposures of H_2O-ice adjacent to the CO_2-ice, based on temperature signatures [Titus *et al.* 2003]. The Observatoire pour la Minéralogie, l'Eau, les Glaces, et l'Activité (OMEGA) observed spectral signatures of both CO_2-ice and trace amounts of H_2O-ice within the residual ice cap [Bibring *et al.* 2004, Douté *et al.* 2007]. OMEGA also confirmed the identification of H_2O-ice-rich surfaces near the CO_2-ice cap

The perennial CO_2 deposit consists of numerous layers. Using Mars Global Surveyor Mars Orbiter Camera (MOC) images, Thomas *et al.* [2005] showed that the south residual cap consists of two distinct layered units, which were deposited at different times, separated by a period of degradation. The older unit, about 10 m thick, has layers approximately 2 m thick. The younger unit has variable numbers of layers, each about 1 m thick.

An estimate of the quantity of CO_2 in the slab, which can be compared to the total CO_2 content of the atmosphere, was made by Byrne and Ingersoll [2003]. They showed that a CO_2 residual ice cap with 10 m thickness, an area of 87,000 km^2, and a density of 1.6 $g.cm^{-3}$, constitutes only about 5% of the average atmospheric mass.

1.2. Surface Reflectivity measured by MARSIS

MARSIS is a decameter-wave sounding radar, which can penetrate kilometers below the icy surface. It has provided important results on the Martian subsurface [Picardi *et al*. 2005; Plaut *et al.* 2007; Watters *et al.* 2007] and ionosphere [Gurnett *et al.* 2005 ; Duru *et al.* 2006; Safaeinili *et al.* 2007; Espley *et al.* 2007]. The radar uses four frequency bands, which are centered at 1.8, 3, 4 and 5 MHz (166, 100, 75, and 60 m wavelength). Each band has a width of 1 MHz.

The data have been corrected for the distortion (phase shift) [Safaeinili *et al. 2003*; Mouginot *et al.* 2008a] and absorption [Mouginot *et al.* 2008b] due to the ionosphere. The radar frequency is close to the plasma frequency (up to4 MHz) of the ionosphere [Nagy *et al.* 2004; Gurnett *et al.* 2005] and as a result the signal is broadened significantly in addition to being delayed. This broadening of the pulses can cause smearing of the resulting radargram. Correction for ionospheric effects is performed to re-sharpen the pulses and compensate for the absorption effects as described in Mouginot *et al.* [2008a].

We quantify the echo returned by the surface from MARSIS radargrams by localizing the position in the radargram corresponding to the surface echo and measuring the amplitude. The position corresponds to the surface elevation given by Mars Orbiter Laser Altimeter (MOLA).

This surface echo amplitude (i.e., surface reflectivity) allows us to build reflectivity maps in each MARSIS frequency band (map at 4 MHz in Fig. 1a; maps at other frequencies show the same type of features). The map resolution is 14.7 km per pixel (about the MARSIS footprint width). For bands centered at 3, 4 and 5 MHz, we used 305, 464 and 539 orbits, respectively, to construct reflectivity maps. For crossing tracks, we average the data from multiple measurements from MARSIS is a nadir-looking radar and the Mars Express polar orbit does not allow us to sound the surface poleward of about 87°N and 87°S; this lack of data results in a gap centered at the pole.

To first order, the reflectivity is inversely correlated with the surface roughness, because the power reflected by a surface at nadir decreases with its roughness. Thus the topographic variations at lateral scales comparable to and/or larger than the MARSIS wavelength are affecting the signal. This is normal behavior due to the loss of coherency of the radar signal.

A simulator of returned radar echoes from Mars was developed by Nouvel et al. [2004]. This computationally efficient radar signal simulation is based on the use of the Facet Method as surface modeling scheme. The slope and the large-scale roughness effects are simulated using MOLA topography to predict the surface echo amplitude in each point [Nouvel et al. 2004]. In this simulation, the reflectivity variability is only due to surface slopes, with an assumption of a single fixed surface dielectric constant. It allows distinguishing dielectric and topographic effects.

For each MARSIS radargram, we generate the corresponding radar simulation and extract the surface amplitude from simulated radargrams to obtain a simulated reflectivity map (Fig. 1b). We use identical procedures to generate both the simulated map and the data map (Fig. 1a).

With such a simulated map, we can correct for any reflectivity variations that are due to topographic effects. Indeed, the reflection coefficient (backscattering coefficient) R can be written as the product of a dielectric constant function and a roughness function [Ulaby et al. 1986], which is independent of the dielectric constant. By normalizing the reflectivity map by the simulated one, we obtain a map proportional to the dielectric constant (Fig. 1c). This normalization consists of the difference of the power logarithms between data and simulated map. This normalized map reveals variations of surface reflectivity across our area of interest. Indeed, one can see that the region of the residual cap has very low reflectivity values (black box in Fig. 1c) compared to the other parts of the SPLD.

2. Wave propagation in a stratified medium

We built a first order model to describe reflectivity in the south residual cap. This model allows us to compute the radar wave propagation in a stratified medium and then obtain a corresponding reflectivity.

Previous work indicates that the south residual cap consists of a thin perennial slab of CO_2-ice overlapping H_2O-ice. So we model the south residual cap reflectivity using three layers: the atmosphere, the CO_2-ice and the H_2O-ice (Fig. 2).

In a two-layer medium with refractive indices n_i and n_j, the reflection coefficient for normal incidence is given by the equation:

$$r_{ij} = \frac{n_j - n_i}{n_j + n_i} \quad (1)$$

In a stratified medium (i.e., with three layers in our case), the reflection coefficient equation may be conveniently expressed in terms of the corresponding coefficients r_{12} and r_{23} associated with the reflection coefficients at the first and the second interface, respectively [Born and Wolf 1959]:

$$r = \frac{r_{12} + r_{23}e^{2i\beta}}{1 + r_{12}r_{23}e^{2i\beta}} \quad (2)$$

where $\beta = \frac{2\pi}{\lambda} n_2 h$, h is the thickness of the intermediate layer and λ is the wavelength of the incident wave. r_{12}, r_{23} may be obtained by substituting equation 1 with the corresponding subscripts. This notation implies that n_1, n_2 and n_3 are respectively, the refractive index for the upper (atmosphere), intermediate (CO_2 slab) and lower (H_2O-ice) layers (see Fig. 2). This model does not include any losses in the media, which, we believe, is a good approximation because for CO_2- and H_2O-ice losses are known to be weak. In addition polar MARSIS measurements typically show low losses [*Plaut et al., 2007*]. The refractive index n_i corresponds to the square root of the real part of dielectric constant: $n_i = \sqrt{\varepsilon_i}$.

As the MARSIS radar signal has a bandwidth of 1 MHz and therefore is not monochromatic, we cannot limit ourselves to equation 2 to obtain the reflectivity. Instead, we have to calculate the reflectivity as:

$$R = \max\left(\left\|\mathrm{IFFT}(S(f)r(f)S^*(f)\right\|^2\right) \quad (3)$$

where *f* is the frequency, *r* is the reflection coefficient defined in equation 2 and *S* is the linearly modulated chirp signal of MARSIS. Equation 3 describes our method to model the amplitude of the surface echo: we apply to an ideal transmitted signal (chirp) the reflection coefficient *r*(*f*). The Inverse Fast Fourier Transform (IFFT) gives a time dependent signal that corresponds to the output of the matched filter of the receiver.

In our model, we describe the H_2O-ice as compact pure water ice, which corresponds to a dielectric constant ε_3 equal to 3.15. This value of pure water ice for the dielectric constant is probably a good assumption, as previous workers have shown that the deposits of the south polar-layered deposits are composed of relatively clean water ice [Plaut *et al.* 2007; Zuber *et al.* 2007]. Moreover laboratory experiments have shown that the real component varies between 3.14 and 3.19 [Ulaby *et al.* 1986] for various types of "dirty ices". In case of porous ice, the dielectric constant decreases. For example, if the porosity of ice were equal to 10%, then, using Maxwell Garnett mixing formulas [Sihvola, 1999], the dielectric constant would be 2.87. The dielectric constant of the atmosphere is set to 1.

Fig. 3 presents the model of reflectivity R as function of the CO_2 thickness, h, for different values of CO_2 dielectric constant. The two free parameters in our model are h and the dielectric constant of the central layer ε_2 (the CO_2-ice). Both have an impact on the inferred reflectivity. The CO_2 thickness in the plot is limited to the 0-20 m range because previous studies have shown that the global thickness is around 10 m.

First, we see on Fig. 3 that the reflectivity is minimal for a layer whose optical thickness $n_2 h$ is close to $\lambda_0 / 4$ (λ_0 is the central wavelength) and the reflectivity is maximal when optical thickness is close to $\lambda_0 / 2$ (Born and Wolf 1979).

Second, the reflectivity is minimum or strictly equal to zero when the dielectric constant of the intermediate layer is equal to $\sqrt{n_1 n_3}$. In our case, this corresponds with a dielectric constant of $\varepsilon_2 \cong 1.77$.

3. Data Analysis

1.3. Comparison to H_2O-ice

As the reflectivity measured by MARSIS is not absolutely calibrated, we have to compare the reflectivity in the south residual cap to a reference region of known composition.

We have chosen a reference region in the SPLD around the position 82°S and 150°W in a 2° by 2° box. It was chosen because of its flatness, so that we can expect that the only parameter that plays a role on the reflectivity is the dielectric constant. We know that the radar waves in the region are reflected by pure water ice, overlain by an optically thin soil layer [*Plaut et al. 2007*]. In this case, the reflection coefficient of the reference region is estimated as $r_{air/H_2O-ice} = 0.279$ with $\varepsilon_{H_2O-ice} = 3.15$ (see equation 1), which corresponds to a reflectivity $R = \left| r_{air/H_2O-ice} \right|^2 = 0.078$.

In our modeling effort, we consider the south residual cap according to the geological unit defined by Skinner *et al.* [2006] in the Mars geologic maps. MARSIS measurements cover about 60% of the 87,000 km^2 the south residual cap (to 87°S). We select all MARSIS reflectivity measurements that are either within the south residual cap or in the reference region. We obtain a distribution (see Fig. 4) of the reflectivity for both regions and for each of the three MARSIS frequency bands. The band 1 centered at 1.8 MHz is not used because of the low amount of data.

In order to find the most probable reflectivity values that characterize each region, we fit this distribution by a Gaussian function. Best-fit parameters are summarized in Table 1. Results show that for all frequencies, the reflectivity is much lower in the south residual cap than in the reference region.

In order to find the best values for model parameters (ε, thickness) that reproduce the observations, we use the model described previously. We fix a range for these parameters, which are from 0 to 20 m for the thickness and from 1.0 to 3.15 for the dielectric constant. The limits for the dielectric constant are the dielectric constant of the upper and lower media (i.e. respectively the atmosphere and the water ice). The procedure consists of a minimization between the model of reflectivity in a stratified medium and the MARSIS measurements for all frequency bands simultaneously.

Application of this procedure gives the best value in our model of a mean thickness of 11 m and a mean dielectric constant of 2.3. This CO_2 dielectric constant is close to the value measured by Pettineli *et al.* [2003] of 2.12. It confirms that the thin bright slab in the south residual cap is primarily CO_2-ice. The formal 1-sigma errors on each parameter, computed from the covariance matrix in the minimization, are 1 m for the thickness and 0.2 for the dielectric constant.

1.4. Local Study

In this section, we are not considering the south residual cap as a single unit, but we try to evaluate, locally, (with a resolution of about 14.7 km) the properties of the CO_2 slab. One can see in Fig. 1c that there is a large variability of reflectivity in the residual cap.

Within our model representation, these variations can be explained as a change in thickness or change in the dielectric constant. In the previous section, we use all the data in the residual cap and so the statistics are robust. This allows us to easily extract the mean behavior. However, in the local study, the statistics for each bin are poor and it is difficult to invert the two parameters at the same time because they play a similar role in reducing the reflectivity of the surface. Alternatively, we can fix one parameter and solve for the other one. Thus for each pixel, we try to describe the reflectivity variation as a change in dielectric constant only, or as a change in CO_2-ice thickness only.

1.1.1. Spatial Variability of the dielectric constant?

First, we fix the thickness at 10 meters and look at the changes in the dielectric constant due to variation of the reflectivity. The resulting dielectric map is shown in Fig. 5a. One can see that the low reflectivity regions (Fig. 1c) correspond to areas where the dielectric constant is close to the value of pure CO_2-ice (2.12) [Pettineli *et al. 2003*]. The central part of the residual cap corresponds to higher values of the dielectric constant, between the CO_2-ice (2.12) and H_2O-ice (3.15) reflectivity values, which means in this case a mixture between H_2O-ice and CO_2-ice. This mixture could be intimate (at the grain size level) or, because MARSIS has a large footprint, CO_2 residual cap and water outcrop reflectivity can be mixed in the returned signal. Using the Maxwell Garnett mixing formula [Sihvola, 1999] and supposing that the effective dielectric constant is only due a mixing between H_2O- and CO_2-ice, we obtain the percentage of CO_2-ice compared to H_2O-ice. Fig. 5a shows that the ice content in the central part could be up to 50% of H_2O, whereas surrounding terrains would contain less than 20%.

1.1.2. Spatial Variability of the thickness?

Next, we fix the CO_2 dielectric constant at 2.12 and estimate the thickness with our model. This CO_2 dielectric constant is close to the previously found value and corresponds to the value measured by Pettineli *et al.* 2003.

Fig. 5b shows the CO_2 thickness computed by our reflectivity model. In this hypothesis, we observe on the Fig. 4b two types of terrains: terrains with relatively low thickness in the central part (less than 6-7m thick) and higher thickness in the surrounding terrains (about 12 m thick). As it is difficult to measure a 1 dB decrease, thicknesses under 4 m cannot be extracted from our analysis.

4. Discussion

1.5. Errors

In this section, we discuss possible errors in our method.

In the first part of the analysis, where we study the general reflectivity of the residual cap, we make an assumption of the constant dielectric of the reference region. For example, if there is a porosity in the shallow subsurface of the ice sheet, the dielectric constant of the reference would decrease and so the reflectivity. For 10% porosity, ε_{H_2O-ice} would be 2.87 and the corresponding reflectivity would be $R = 0.066$. A porosity of 10% in water ice would thus reduce the reflectivity less than 1 dB.

Our model assumes no porosity for water ice (i.e. $\varepsilon_{H_2O-ice} = 3.15$) and we think that the assumption does not have a significant effect on our results. Our model is not particularly sensitive to this parameter. For the 10%-porosity case, the output values of the model would be still 11 m for the thickness and 2.2 for the dielectric constant of the CO2. This change is inside the uncertainties given by the 1-sigma errors on each parameter.

In the second part, where we study the spatial variability in the south residual cap, we cannot exclude that the effect of roughness at about tens of meters scale could explain the reflectivity variability. However we think that the geologic features in the residual cap (depressions of few meters) are small compared to the MARSIS wavelength and are not responsible for the decrease in reflectivity.

1.6. Conclusions

The multi-layered reflection model proposed in this paper allows us to estimate a CO_2 slab thickness for a portion of the south residual cap of Mars. The mean CO_2 thickness measured by MARSIS seems to be in agreement with the thickness estimated by Thomas *et al.* 2005.

It is interesting to note that the reflectivity detected by MARSIS is not homogenous across the residual cap. Indeed we observe that the central part of the residual cap has higher reflectivity than surrounding areas.

We have proposed an interpretation of this heterogeneity in terms of dielectric constant and thickness of the CO_2-ice slab.

Firstly, supposing that the thickness is constant across the residual cap and solving for dielectric variations, we would conclude that the central part is a mixture of CO_2 and H_2O ices, and the surrounding terrains are mainly pure CO2-ice.

Alternatively, supposing that the residual cap composition is homogeneously pure

CO2-ice and solving for thickness variations, it appears that the central terrains are thinner that the surrounding terrains. In this case, the volume of CO_2-ice contained in the mapped part of the residual cap is about 4.1x10^{11} m^3. As MARSIS measurements cover 60% of the residual cap, we can estimate that the total volume 6.85x10^{11} m^3, which corresponds to about 5% (0.27 mbar) of atmospheric surface pressure (5.6 mbar) if we assume that the CO_2–ice density is about 1.6 g.cm^3. This estimation is consistent with previous works that predict that the amount of CO2 in the residual cap is small compared to the mass of the atmosphere [Prettyman *et al.* 2004*;* Byrne and Ingersoll, 2003].

In both cases, our model shows that the central part of the mapped portion of the residual cap, which shows lower surface reflectivity, contains less CO_2-ice than the surrounding parts of the residual cap.

A similar analysis could be conducted with the SHAllow subsurface RADar (SHARAD), which operates at 20 MHz (i.e., a wavelength of 15 m in vacuum). The SHARAD horizontal resolution is 300 m, which would allow description of the surface features at a better resolution. SHARAD may also be sensitive to the seasonal CO_2 deposits when the thickness is 1-2 m as described by Nunes and Phillips 2006., although this study is probably more difficult because SHARAD is more sensitive to meter-scale roughness.

Acknowledgments

The authors acknowledge the French space agency (CNES) for support of these studies in Laboratoire de Planétologie de Grenoble. Operations of the Mars Express spacecraft by the European Space Agency (ESA) are gratefully acknowledged. Lynn Carter and an anonymous reviewer provided helpful suggestions for this paper.

References

Bibring, J., and 13 colleagues, 2004. Perennial water ice identified in the south polar cap of Mars , Nature 428, 627-630.

Born M. and Wolf E., 1979. Principles of Optics: Electromagnetic theory of propagation, interference and diffraction of light, Cambridge Univ. Press, Cambridge, UK.

Byrne, S. and Ingersoll, A. P., 2003. A Sublimation Model for Martian South Polar Ice Features, Science 299, 1051-1053.

Douté, S. Schmitt, B., Langevin, Y., Bibring, J.-P., Altieri, F., Bellucci, G., Gondet, B., Poulet, F. & the MEX OMEGA team, 2007. South Pole of Mars: Nature and composition of the icy terrains from Mars Express OMEGA observations, Planetary And Space Science 55, 113-133.

Duru, F.; Gurnett, D. A.; Averkamp, T. F.; Kirchner, D. L.; Huff, R. L.; Persoon, A. M.; Plaut, J. J. & Picardi, G., 2006. Magnetically controlled structures in the ionosphere of Mars, J. Geophys. Res. 111, A12204.

Espley, J. R., Farrell, W. M., Brain, D. A., Morgan, D. D., Cantor, B., Plaut, J. J., Acuña, M. H., Picardi, G., 2007. Absorption of MARSIS radar signals: Solar energetic particles and the daytime ionosphere, Geoph. Res. Let. 34, 9101-+.

Flammarion, C., 1892. La planète mars et ses conditions d'habitabilité, v. 1. Gauthier–Villars et Fils, Paris.

Gurnett, D.A. and 11 colleagues, 2005. Radar soundings of the ionosphere of Mars, Science 310, 1929–1933.

Kieffer, H.H., 1979. Mars south polar spring and summer temperatures: a residual CO2 frost, J. Geophys. Res. 84, 8263–8288.

Mouginot, J.; Kofman, W.; Safaeinili, A.; Herique, 2008a. A Correction of the ionospheric distortion on the MARSIS surface sounding echoes, Planetary and Space Science 56, 917-926.

Mouginot, J.; Kofman, W.; Safaeinili, A.; Herique, A.; Plaut, J. J.; Picardi, G., 2008b. Calibration of MARSIS Surface Echoes LPSC XXXIX, No. 1391, p. 1716

Nouvel, J. F.; Herique, A.; Kofman, W., Safaeinili, A., 2004. A. Radar signal simulation: Surface modeling with the Facet Method, Radio Science 39, RS1013.

Nunes, D. C., Phillips, R. J., 2006. Radar Subsurface Mapping of the Polar Layered Deposits on Mars J. Geophys. Res. 111, 6+-.

Paige, D., Herkenhoff, K., Murray, B., 1990. Mariner 9 observations of the south polar cap of Mars: evidence for residual CO2 frost. J. Geophys. Res. 95, 1319–1335.

Pettinelli, E.; Vannaroni, G.; Cereti, A.; Paolucci, F.; Della Monica, G.; Storini, M. & Bella, F., 2003. Frequency and time domain permittivity measurements on solid CO_2 and solid CO_2-soil mixtures as Martian soil simulants, J. Geophys. Res. 108, 10-+

Picardi, G. and 12 colleagues, 2004. Performance and surface scattering models for the Mars Advanced Radar for Subsurface and Ionosphere Sounding (MARSIS) Planet. and Space Science 52, 149-156.

Plaut, J. J.and 23 colleagues, 2007. Subsurface Radar Sounding of the South Polar Layered Deposits of Mars, Science 316, 92-.

Prettyman, T. H. and 12 colleagues, 2004. Composition and structure of the Martian surface at high southern latitudes from neutron spectroscopy, J. Geophys. Res. 109, 5001-+

Safaeinili, A.; Kofman, W.; Nouvel, J.; Herique, A., Jordan, R. L., 2003. Impact of Mars ionosphere on orbital radar sounder operation and data processing, Planetary and Space Science 51, 505-515.

Safaeinili, A.; Kofman, W.; Mouginot, J.; Gim, Y.; Herique, A.; Ivanov, A. B.; Plaut, J. J., Picardi, G., 2007. Estimation of the total electron content of the Martian ionosphere using radar sounder surface echoes, Geophysical Reseach Letters 34, 23204-+.

Skinner, J.A., Jr., Hare, T.M., Tanaka, K.L., 2006, Digital Renovation of the Atlas of Mars 1:15,000,000-Scale Global Geologic Series Maps, LPSC XXXVII, abstract #2331

Sihvola A. , 1999. Electromagnetic mixing formulas and applications, IEE Electromagnetic waves series 47, The institution of Electrical Engineers.

Ulaby, F.T., Moore, R.K., Fung, A.K., 1986. Microwave Remote Sensing Active and Passive, Artech House, Volume II.

Watters, T. R. and 12 colleagues, 2007. Radar Sounding of the Medusae Fossae Formation Mars: Equatorial Ice or Dry, Low-Density Deposits? Science, 318, 1025.

Zuber, M. T.; Phillips, R. J.; Andrews-Hanna, J. C.; Asmar, S. W.; Konopliv, A. S.; Lemoine, F. G.; Plaut, J. J.; Smith, D. E. & Smrekar, S. E., 2007. Density of Mars South Polar Layered Deposits, Science 317, 1718-.

Tables

Center of the Gaussian	3 MHz	4 MHz	5 MHz
South residual cap	-13.1	-14.1	-15.5
Surface reference [H_2O-ice]	-7.5	-8.5	-8.3
Reflectivity decrease	5.6	5.5	7.2

Table Captions

Table 1: The table summarizes the result of the Gaussian fit made on the distribution presented in Fig. 4. The two first lines show the reflectivity (in dB) of the central position of the Gaussian (for the residual cap and for the reference region, respectively). The last line corresponds to the difference (in dB) between reference and residual cap.

Figure Captions

Fig. 1: (a) Surface reflectivity map from MARSIS using the radar frequency centered at 4 MHz. The projection is polar stereographic. The reflectivity is represented in decibel scale. (b) Simulated reflectivity map using MOLA topography. The simulation is performed with a constant $\varepsilon_{surface}$. (c) Surface reflectivity map at 4 MHz normalized by the simulated reflectivity map. (d) Mars Orbiter Camera (MOC) wide-angle mosaic map of the south polar region of Mars. The map resolution is about 14.7 km per pixel.

Fig. 2: Schematic view of a vertical ground section of the south residual cap, as described in our model.

Fig. 3: Reflectivity R of the layered surface (see Fig. 2) as a function of the thickness h for different values of the dielectric constant ε_{CO_2}. The dielectric constants of the upper and lower medium are 1 and 3.15, respectively.

Fig. 4: The distribution of surface reflectivity in the reference region (dark grey) and the south residual cap (light grey). The black dashed lines are the Gaussian fit made on the distribution. The results of the fit are summarized in Table 1.

Fig. 5: Maps of the south residual cap region. (a) Map of the dielectric constant found by our reflectivity model with the thickness fixed at 10 meters. Using the Maxwell Garnett mixing formula [Sihvola, 1999] and assuming that the effective dielectric

constant is only due to mixing between H_2O- and CO_2-ice, we give the percentage of CO_2-ice and H2O-ice. (b) Map of the CO_2 thickness found by our model with dielectric constant fixed at 2.12.

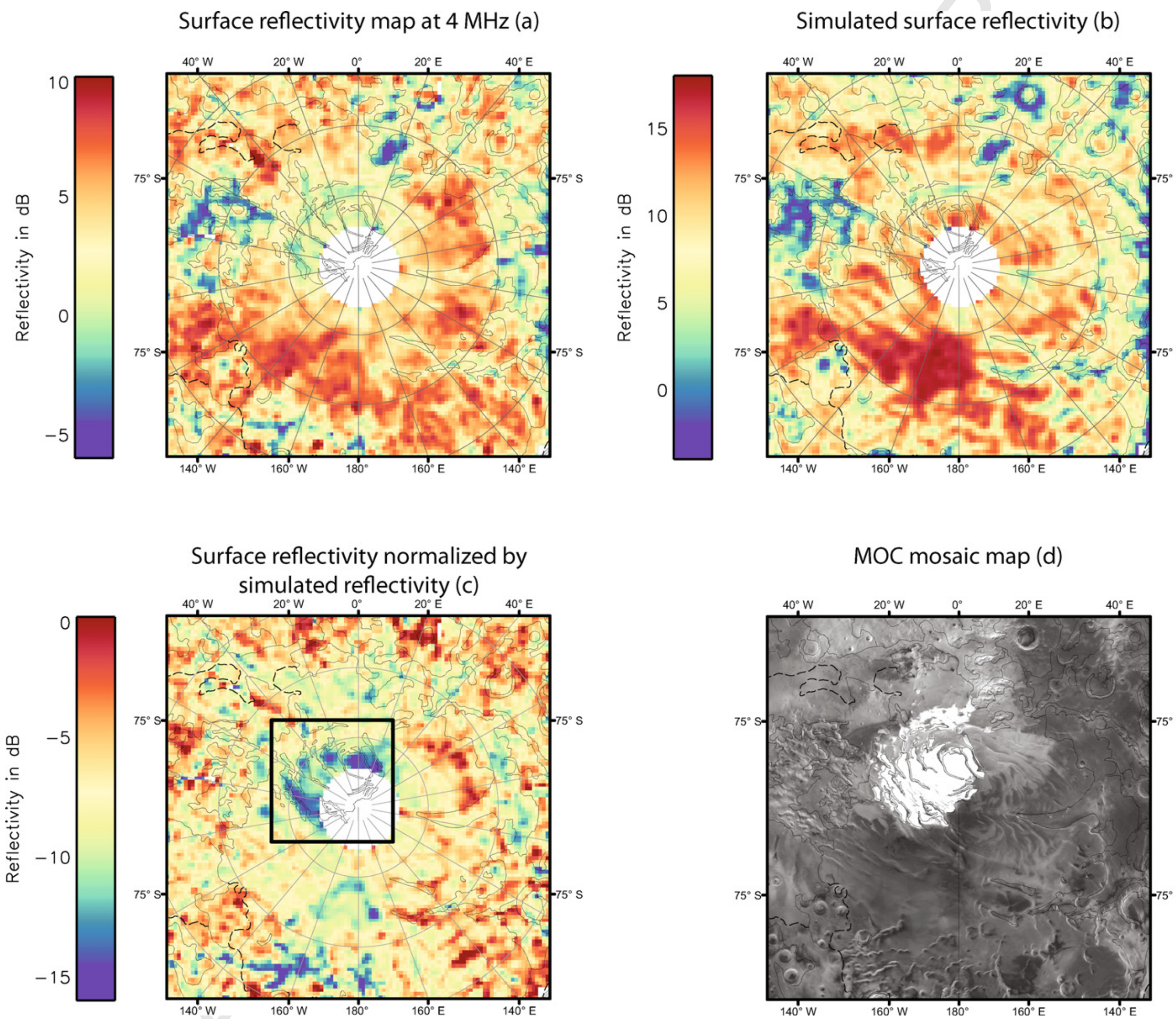

Surface reflectivity map at 4 MHz (a)
Simulated surface reflectivity (b)
Surface reflectivity normalized by simulated reflectivity (c)
MOC mosaic map (d)
Reflectivity in dB
40° W
20° W
0°
20° E
40° E
75° S
140° W
160° W
180°
160° E
140° E
10
5
0
−5
15
−10
−15

I10547_fig1

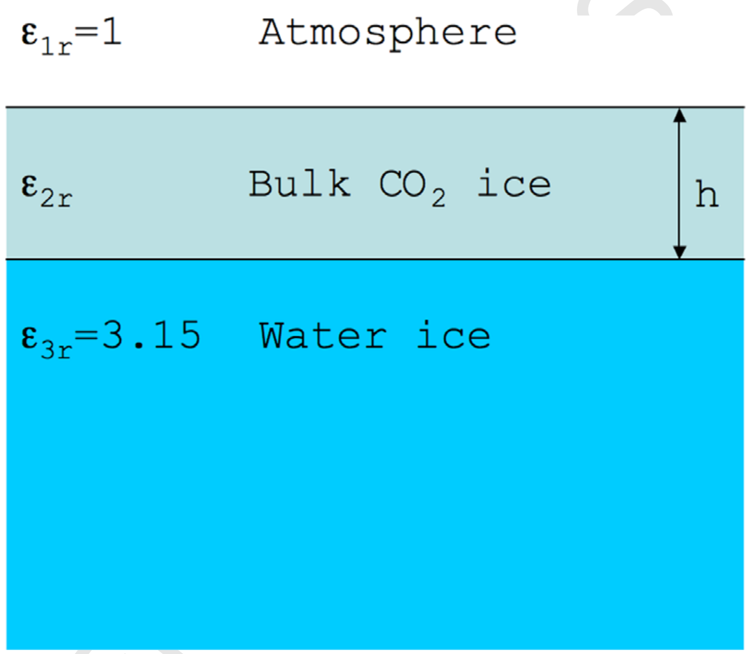

ε_{1r}=1 Atmosphere
ε_{2r} Bulk CO_2 ice
h
ε_{3r}=3.15 Water ice

I10547_fig2

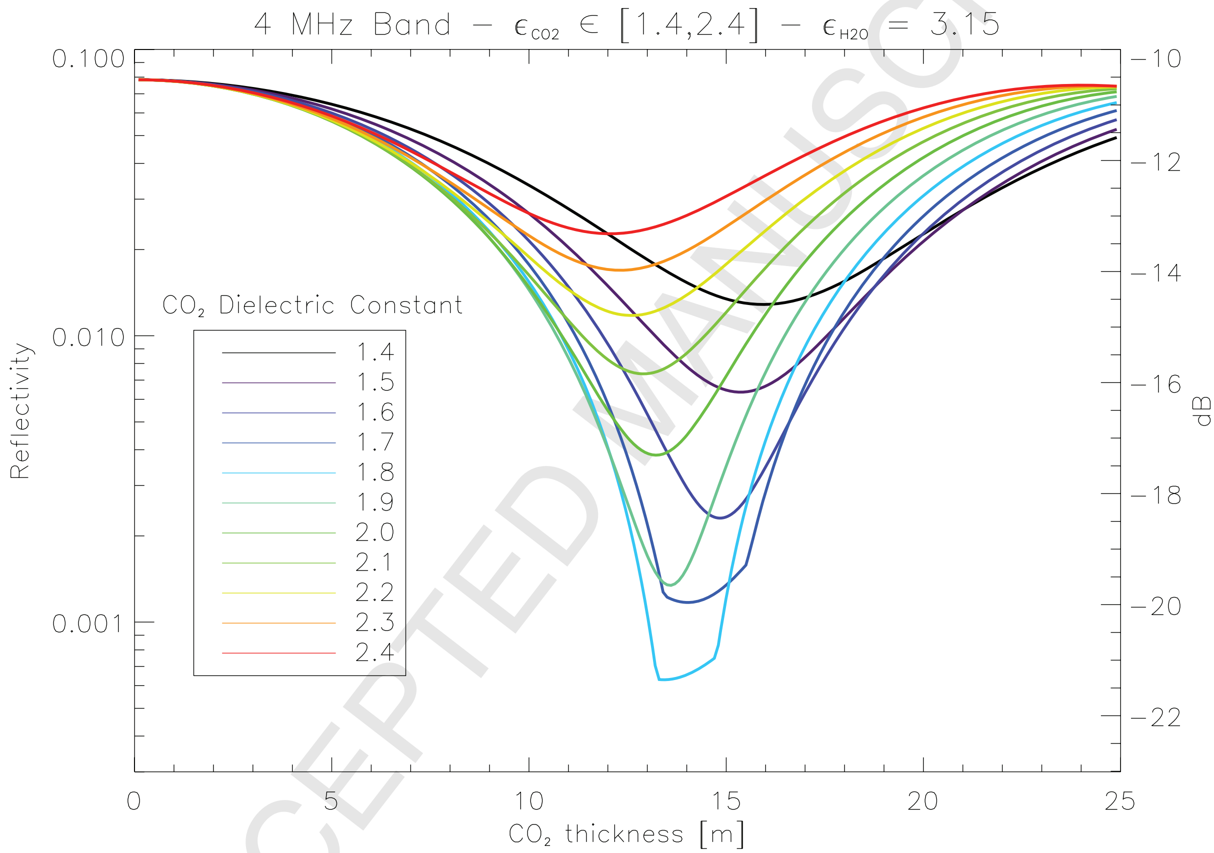

4 MHz Band – ϵCO2 ∈ [1.4,2.4] – ϵH2O = 3.15
0.100
0.010
0.001
Reflectivity
−10
−12
−14
−16
−18
−20
−22
dB
0
5
10
15
20
25
CO2 thickness [m]
CO2 Dielectric Constant
1.4
1.5
1.6
1.7
1.8
1.9
2.0
2.1
2.2
2.3
2.4

I10547_fig3

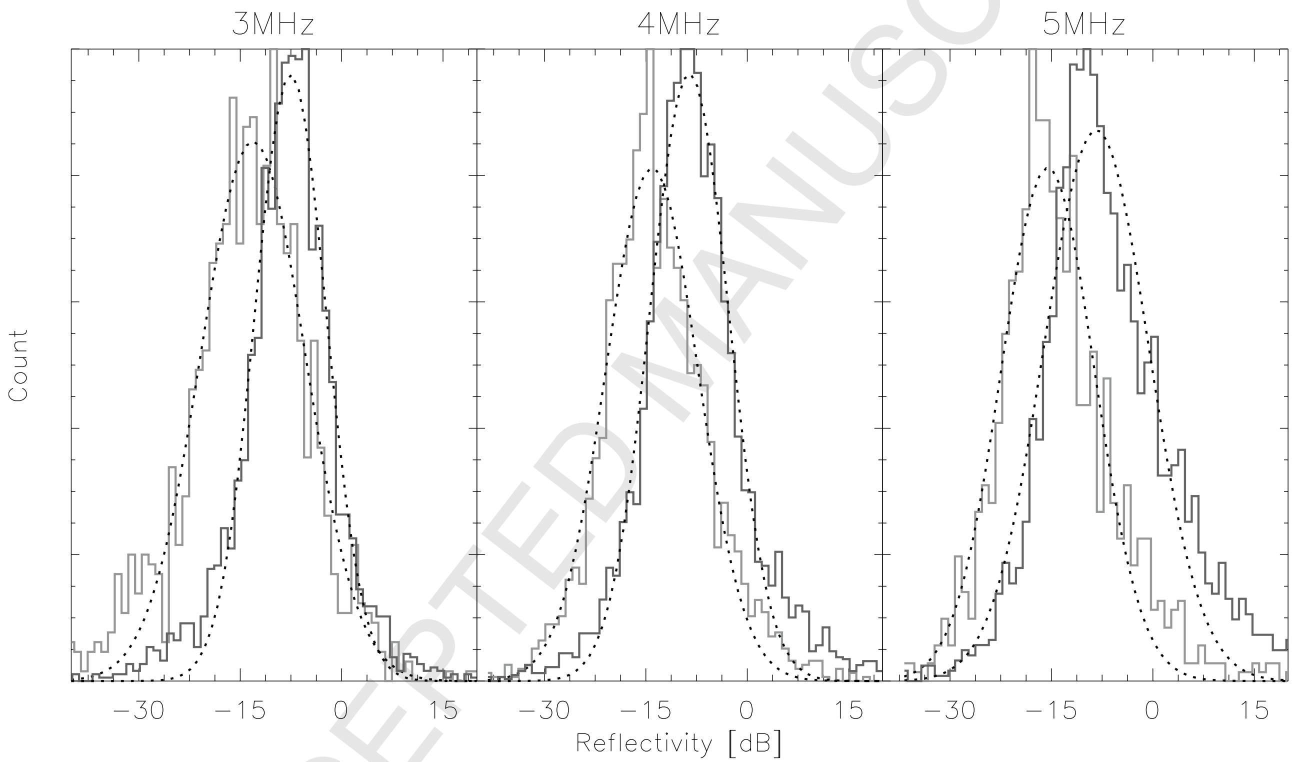
3MHz
4MHz
5MHz
Count
−30 −15 0 15
−30 −15 0 15
−30 −15 0 15
Reflectivity [dB]

I10547_fig4

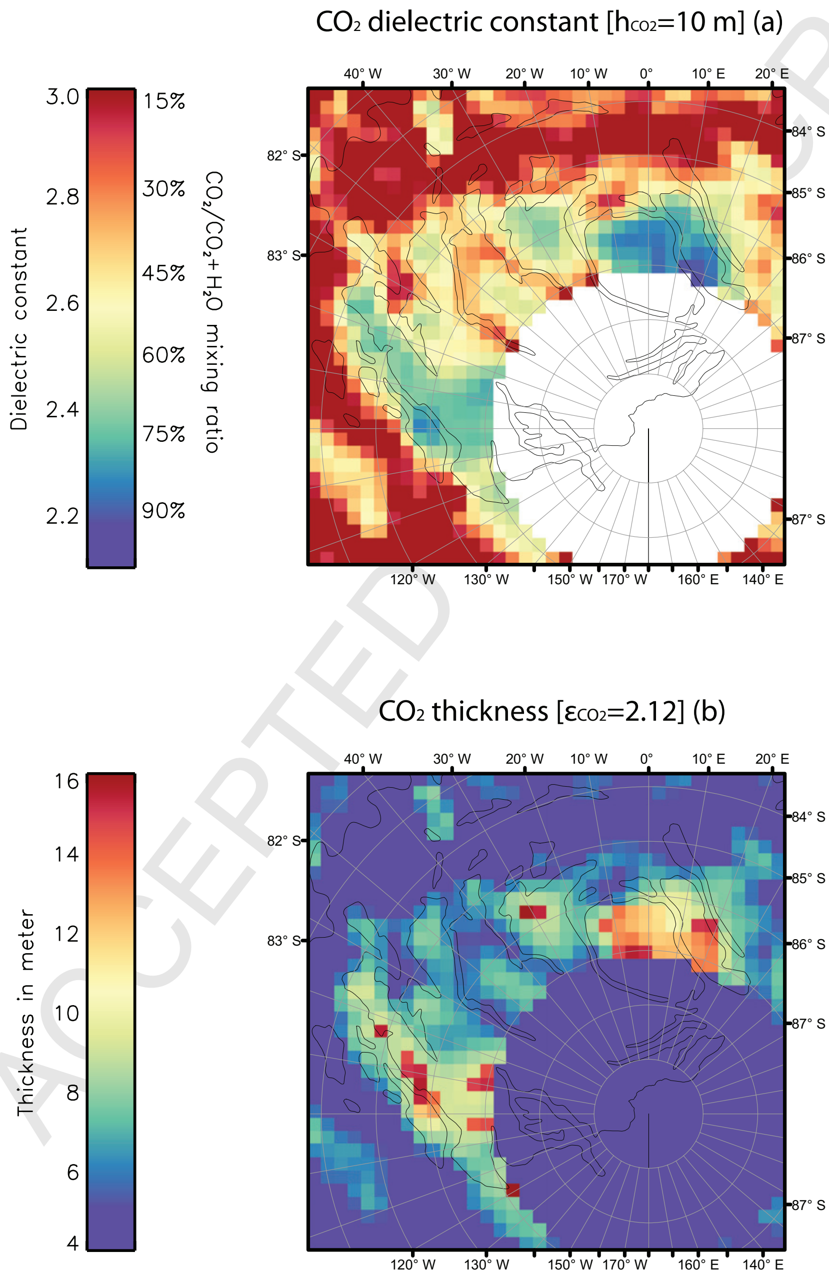

Figure 5 - Mouginot (2008)

I10547_fig5